

Phase Investigations in the System Na_3AlF_6 - Li_3AlF_6

J. L. HOLM and B. JENSSEN HOLM

*Institute of Inorganic Chemistry, The Technical University of Norway,
N-7034 Trondheim — NTH, Norway*

The system Na_3AlF_6 - Li_3AlF_6 has been examined by differential thermal analysis (DTA), and by X-ray diffraction studies at different temperatures.

Two intermediate compounds, corresponding to $\text{Na}_2\text{LiAlF}_6$ and $\text{Na}_3\text{Li}_3\text{Al}_2\text{F}_{13}$ were found, the latter identical with the cubic mineral cryolithionite. $\text{Na}_2\text{LiAlF}_6$ was found to be monoclinic at room temperature, with $a=7.538$ Å, $b=7.516$ Å, $c=7.525$ Å, $\beta=90.81^\circ$ (20°C). On heating, the monoclinic α - $\text{Na}_2\text{LiAlF}_6$ modification is changed to cubic β - $\text{Na}_2\text{LiAlF}_6$, $a=7.639$ Å (445°C).

No solid solution was found at room temperature, while extensive formation of solid solutions was observed at higher temperatures.

The liquidus curve has its minimum at 710°C and 64 mole % Li_3AlF_6 . One new phase was found between 560°C and 660°C , 90 and 99 mole % Li_3AlF_6 . This phase is tetragonal, with $a=11.97$ Å, $c=8.73$ Å (625°C).

The system Na_3AlF_6 - Li_3AlF_6 , sodium cryolite-lithium cryolite, is of interest both from a theoretical, and from a more applied, industrial point of view.

It is of interest to get the phase conditions established correctly, especially because the system is formed by two complex compounds both showing interesting polymorphic behavior in the solid state. Furthermore, two minerals, cryolite, Na_3AlF_6 , and cryolithionite, $\text{Na}_3\text{Li}_3\text{Al}_2\text{F}_{12}$, can be formed from the constituents in this system. Both of these have been found in the famous deposits at Ivigtut, Greenland.

Besides its theoretical and mineralogical interest, the phase diagram is of interest because of its connection to the aluminium electrolysis. Minor amounts of LiF or Li_3AlF_6 may be added to the commercial electrolyte ($\text{Na}_3\text{AlF}_6 + \text{Al}_2\text{O}_3$) in order to improve the electrical conductivity and to lower the melting point and the density of the bath.

During the last 30 years, the system has been examined by several investigators,¹⁻⁷ resulting in widely divergent conclusions. Drossbach¹ (1937) assumed a continuous series of solid solutions throughout the system just below the liquidus curve. Mashovets and Petrov² (1957), however, reported a simple eutectic system with no solid solution. A later work (1964) by Rolin

and Muhlethaler³ partly confirmed Drossbach's results. These authors found a eutectic point at 62.3 mole % Li_3AlF_6 , 713°C, with solid solution extending to the eutectic point on the Li_3AlF_6 side, and to 36 mole % Li_3AlF_6 on the Na_3AlF_6 side. This was confirmed, by high-temperature X-ray and DTA studies, by Holm⁸ (1966) who reported solid solution on both sides in the system. Solid solution on both sides was also found by Babayan and co-workers⁵ (1967).

Beletskii and Saksonov⁹ (1957) studied the system at room temperature by X-ray diffraction. They reported that three compounds, $\text{Na}_6\text{Li}_3\text{Al}_3\text{F}_{18}$, $\text{Na}_3\text{Li}_6\text{Al}_3\text{F}_{18}$, and $\text{Na}_3\text{Li}_{15}\text{Al}_6\text{F}_{36}$ were formed in the system. They did not find any compound of the composition $\text{Na}_3\text{Li}_3\text{Al}_2\text{F}_{12}$, corresponding to the mineral cryolithionite. Holm¹⁰ (1963), however, fused Li_3AlF_6 and Na_3AlF_6 in molar proportions 1:1, and by this method obtained a product identical to cryolithionite. This result was later confirmed by Garton and Wanklyn⁶ (1967), who examined the system by means of X-ray diffraction at room temperature, including studies of quenched samples, and by DTA. At room temperature they found two compounds, $\text{Na}_2\text{LiAlF}_6$ and $\text{Na}_3\text{Li}_3\text{Al}_2\text{F}_{12}$ (cryolithionite). At higher temperatures they report several phases. These latter results, however, were based on studies of quenched samples. We have found that the method of quenching may very easily give misleading results in this system. This is probably due to the fact that some of the transformations or phase changes are so rapid that the high-temperature phases will not be preserved by quenching. Also, some modifications pass through metastable intermediate forms on cooling, and these forms may be preserved by quenching (*cf.* our studies of Li_3AlF_6 ¹¹).

EXPERIMENTAL

Sodium cryolite was hand-picked, natural cryolite from Ivigtut, Greenland. Lithium cryolite was made by fusing AlF_3 and LiF in molar proportions 1:3. The aluminium fluoride was prepared by repeated vacuum sublimation of technical grade AlF_3 (Riedel de Haën AG, Germany). The lithium fluoride (Fisher Certified Reagent, Fisher, USA) was dried in a vacuum furnace at 400°C, and then melted before use. Clear crystals were selected from the samples. Samples for the X-ray investigations were prepared by fusing Li_3AlF_6 and Na_3AlF_6 in the desired proportions.

DTA was carried out in a furnace of the standard type as used in our institute, described by Motzfeldt.¹² The sample and reference (Al_2O_3 , fired at 1100°C) were placed in platinum crucibles mounted in a nickel block. The temperature and differential temperature were measured by Pt/Pt10 % Rh thermocouples. The DTA curves were recorded partly by an X-Y recorder (Speedomax G, Leeds & Northrup, USA) and partly by a Varian G 2022 Dual Channel Recorder. In both cases the signal was amplified by use of a DC Microvolt Amplifier, range 50–2000 μV (Leeds & Northrup, USA).

The X-ray experiments were carried out in a metal ribbon furnace, similar to the type described by Smith.¹³ The heating element was a flat strip made from platinum-10 % rhodium. The temperature was recorded with a Pt/Pt10 % Rh thermocouple welded to the strip, and was constant within $\pm 1^\circ\text{C}$ with time. Calibration at the transition point of NaAlF_6 ($\alpha \rightarrow \beta$) at 560°C showed the recorded temperature to be correct to within $\pm 5^\circ\text{C}$. The radiation used was nickel-filtered $\text{CuK}\alpha$, and the X-ray diagrams were recorded by a Philips diffractometer (basic unit, PW 1353/00).

The DTA and X-ray equipment has been described in detail elsewhere.¹⁴ All high-temperature work was carried out in an atmosphere of purified nitrogen (99.99 % N_2 , Norsk Hydro, Norway). Complete exclusion of air and humidity is especially important

when working in this system, in order to avoid formation of lithium aluminate, LiAl_5O_8 . This compound is cubic, with $a=7.93 \text{ \AA}$,¹⁵ and may therefore easily be confused with $\beta\text{-Na}_3\text{AlF}_6$, though there are a few dissimilarities in the powder diagrams of the two compounds.

The density measurements were carried out at 25°C by a vacuum pycnometric method, using Shell Odourless Kerosene as the displacement liquid.

RESULTS AND DISCUSSION

a) DTA examinations. During DTA runs, both heating and cooling curves were recorded. The heating rate was 5°C/min and the cooling rate 2–3°C/min. By use of our DTA equipment, it is possible to detect solidus curves in systems where the solid solubility exceeds 10–20 mole %. The system KCl–NaCl, in which a continuous series of solid solutions is formed,^{16–18} was selected as a model. Examination by DTA showed that both the solidus and the liquidus curve, as well as the miscibility gap, could be detected by this method. Examples of DTA curves from this system are shown in Fig. 1. As can be seen,

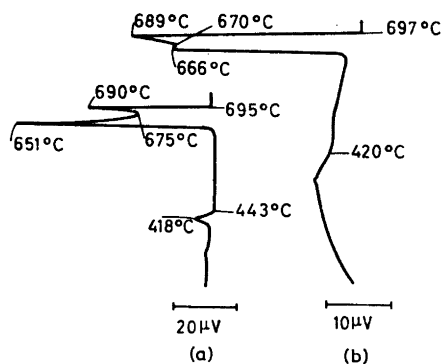


Fig. 1. DTA cooling curves from the system NaCl–KCl. Differential temperature versus temperature. (a) 33.4 mole % KCl; liquidus point 695°C, solidus point 675°C, critical mixing point 443°C. (b) 70.2 mole % KCl; liquidus point 697°C, solidus point 670°C, critical mixing point 420°C.

the diagrams show separate and well established peaks at temperatures corresponding to both the liquidus point and the solidus point in the system. These diagrams are very similar to those found in the system Na_3AlF_6 – Li_3AlF_6 . Examples of DTA curves from the latter system are given in Fig. 2.

The reaction temperatures used in the phase diagram (Fig. 3) were mainly taken from the cooling curves, as the use of heating curves in this case led to much larger uncertainties in the temperature determination. However, the uncertainty in establishing the temperature where the last part of the melt disappears (the solidus point), was always much larger than the uncertainty in establishing the temperature of the first appearance of solid (the liquidus point).

By DTA one or two small peaks were sometimes observed in the temperature range 650–680°C, especially on the Na_3AlF_6 side of the system. By X-ray examination of samples in this temperature region, we could not detect any phase change which could support these peaks in the DTA-diagrams. We think these peaks must be due to evaporation from the system, which will

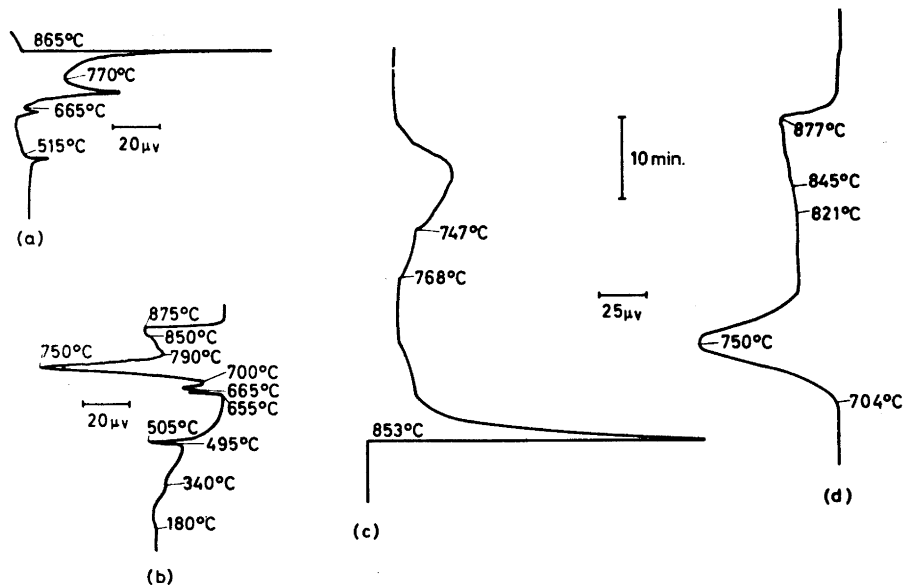


Fig. 2. DTA curves from the system Na_3AlF_6 – Li_3AlF_6 , 33.3 mole % Li_3AlF_6 . (a) and (b) Differential temperature *versus* temperature (from XY-recorder). (c) and (d) Differential temperature *versus* time (from dual channel recorder). (a) and (c) are heating curves, (b) and (d) are cooling curves.

lead to a change in composition from the binary system Na_3AlF_6 – Li_3AlF_6 to the ternary system Na_3AlF_6 – Li_3AlF_6 – LiF . No reliable determination of the boundary curves and ternary point in this system is known.

b) X-Ray examinations. Samples with the following compositions were studied by X-ray diffraction at room temperature: 0, 10, 25, 33.3, 40, 50.0, 56, 70, 80, 90, and 100 mole % Li_3AlF_6 . Two intermediate compounds, α - $\text{Na}_2\text{LiAlF}_6$ and $\text{Na}_3\text{Li}_3\text{Al}_2\text{F}_{12}$, were found. No peak shifts which might indicate formation of solid solutions at room temperature were observed.

A number of samples were examined by X-ray at higher temperatures. A survey of these examinations, and the results that were found, are given in Table 1. Some of the transformations observed on heating were fairly slow, *e.g.* the transformation to β -cryolite solid solution. At 625°C most samples reached their final structure only after 1–4 h.

c) The compound $\text{Na}_2\text{LiAlF}_6$. The compound $\text{Na}_2\text{LiAlF}_6$ was found to be monoclinic B-face-centered at room temperature, with the lattice parameters $a = 7.538 \text{ \AA}$, $b = 7.516 \text{ \AA}$, $c = 7.525 \text{ \AA}$, $\beta = 90.81^\circ$ (20°C). Powder pattern data for α - $\text{Na}_2\text{LiAlF}_6$ are given in Table 2. The density was measured to 3.03 g/cm³, which is in very good agreement with the calculated value of 3.021 g/cm³ (4 formula units in the unit cell).

There is good agreement between the d -values of α - $\text{Na}_2\text{LiAlF}_6$ found by us and those reported by Garton and Wanklyn.⁶ We believe, however, that their indexing on the basis of a hexagonal unit cell is erroneous, as it is not

Table 1. High-temperature X-ray examinations in the system Na_3AlF_6 - Li_3AlF_6 .

Measurement No.	Mole % Li_3AlF_6	Temp. (°C)	Observed phases, with lattice constants. ss denotes solid solution.
1	0	625	$\beta\text{-Na}_3\text{AlF}_6$, $a=7.967 \pm 0.004 \text{ \AA}$
2	10	625	$\beta\text{-Na}_3\text{AlF}_6$, $a=7.97 \pm 0.01 \text{ \AA}$
3	25	625	$\beta\text{-Na}_3\text{AlF}_6(\text{ss})$, $a=7.967 \pm 0.007 \text{ \AA}$
4	33.33	445	$\beta\text{-Na}_2\text{LiAlF}_6$, $a=7.639 \pm 0.005 \text{ \AA}$
5	»	480	$\beta\text{-Na}_2\text{LiAlF}_6$, $a=7.655 \pm 0.006 \text{ \AA}$
6	»	500	$\beta\text{-Na}_2\text{LiAlF}_6$, $a=7.67 \pm 0.01 \text{ \AA}$
7	»	520	$\beta\text{-Na}_2\text{LiAlF}_6(\text{ss})$, $a=7.76 \pm 0.01 \text{ \AA}$ + $\beta\text{-Na}_3\text{AlF}_6(\text{ss})$, $a=7.90 \pm 0.01 \text{ \AA}$
8	»	530	$\beta\text{-Na}_3\text{AlF}_6(\text{ss})$, $a=7.94 \pm 0.01 \text{ \AA}$
9	»	625	$\beta\text{-Na}_3\text{AlF}_6(\text{ss})$, $a=7.940 \pm 0.001 \text{ \AA}$
10	40	445	$\beta\text{-Na}_2\text{LiAlF}_6$, $a=7.60 \pm 0.02 \text{ \AA}$ + $\text{Na}_3\text{Li}_3\text{Al}_2\text{F}_{12}$, $a=12.245 \pm 0.006 \text{ \AA}$
11	»	520	$\beta\text{-Na}_2\text{LiAlF}_6$, $a=7.63 \pm 0.01 \text{ \AA}$ + $\text{Na}_3\text{Li}_3\text{Al}_2\text{F}_{12}$, $a=12.27 \pm 0.03 \text{ \AA}$
12	»	545	$\beta\text{-Na}_2\text{LiAlF}_6$, $a=7.64 \pm 0.02 \text{ \AA}$ + $\text{Na}_3\text{Li}_3\text{Al}_2\text{F}_{12}$, $a=12.26 \pm 0.02 \text{ \AA}$
13	»	625	$\beta\text{-Na}_3\text{AlF}_6(\text{ss})$, $a=7.97 \pm 0.01 \text{ \AA}$
14	»	690	$\beta\text{-Na}_3\text{AlF}_6(\text{ss})$, $a=7.974 \pm 0.006 \text{ \AA}$
15	45	480	$\beta\text{-Na}_2\text{LiAlF}_6$, $a=7.665 \pm 0.04 \text{ \AA}$ + $\text{Na}_3\text{Li}_3\text{Al}_2\text{F}_{12}$, $a=12.33 \pm 0.01 \text{ \AA}$
16	»	525	$\beta\text{-Na}_2\text{LiAlF}_6$, $a=7.685 \pm 0.008 \text{ \AA}$ + $\text{Na}_3\text{Li}_3\text{Al}_2\text{F}_{12}$, $a=12.33 \pm 0.01 \text{ \AA}$
17	50	450	$\text{Na}_3\text{Li}_3\text{Al}_2\text{F}_{12}$, $a=12.271 \pm 0.003 \text{ \AA}$
18	»	550	$\text{Na}_3\text{Li}_3\text{Al}_2\text{F}_{12}(\text{ss})$, $a=12.30 \pm 0.01 \text{ \AA}$ + $\beta\text{-Na}_2\text{LiAlF}_6$, $a=7.679 \pm 0.003 \text{ \AA}$
19	»	625	$\beta\text{-Na}_3\text{AlF}_6(\text{ss})$, $a=7.954 \pm 0.006 \text{ \AA}$
20	59	625	$\beta\text{-Na}_3\text{AlF}_6(\text{ss})$, $a=7.963 \pm 0.006 \text{ \AA}$
21	62.3	625	$\beta\text{-Na}_3\text{AlF}_6(\text{ss})$, $a=7.98 \pm 0.01 \text{ \AA}$
22	64.5	625	$\text{Na}_3\text{Li}_3\text{Al}_2\text{F}_{12}(\text{ss})$, $a=12.30 \pm 0.02 \text{ \AA}$ + $\beta\text{-Na}_3\text{AlF}_6(\text{ss})$, $a=7.95 \pm 0.03 \text{ \AA}$
23	70	625	$\text{Na}_3\text{Li}_3\text{Al}_2\text{F}_{12}(\text{ss})$, $a=12.31 \pm 0.01 \text{ \AA}$ + $\beta\text{-Na}_3\text{AlF}_6(\text{ss})$, $a=7.95 \pm 0.03 \text{ \AA}$
24	80	550	$\gamma\text{-Li}_3\text{AlF}_6(\text{ss}) + \text{Na}_3\text{Li}_3\text{Al}_2\text{F}_{12}(\text{ss})$
25	»	625	$\text{Na}_3\text{Li}_3\text{Al}_2\text{F}_{12}(\text{ss})$, $a=12.30 \pm 0.03 \text{ \AA}$ + $\beta\text{-Na}_3\text{AlF}_6(\text{ss})$, $a=7.97 \pm 0.02 \text{ \AA}$
26	83.5	625	$\text{Na}_3\text{Li}_3\text{Al}_2\text{F}_{12}(\text{ss})$, $a=12.30 \pm 0.04 \text{ \AA}$
27	90	625	$\text{Na}_3\text{Li}_3\text{Al}_2\text{F}_{12}(\text{ss})$, $a=12.30 \pm 0.04 \text{ \AA}$
28	92	610	Tetragonal phase
29,30	»	620-640	Tetragonal phase + $\text{Na}_3\text{Li}_3\text{Al}_2\text{F}_{12}(\text{ss})$, $a=12.23 \pm 0.07 \text{ \AA}$ (625°C)
31	»	> 640	$\text{Na}_3\text{Li}_3\text{Al}_2\text{F}_{12}(\text{ss})$
32	95	550	$\gamma\text{-Li}_3\text{AlF}_6(\text{ss}) + \text{Na}_3\text{Li}_3\text{Al}_2\text{F}_{12}(\text{ss})$ (small amounts)
33	»	625	Tetragonal phase, $a=11.97 \pm 0.02 \text{ \AA}$, $c=8.73 \pm 0.02 \text{ \AA}$ + traces of $\text{Na}_3\text{Li}_3\text{Al}_2\text{F}_{12}(\text{ss})$
34-36	»	640-660	Tetragonal phase + $\text{Na}_3\text{Li}_3\text{Al}_2\text{F}_{12}(\text{ss})$
37	»	> 660	$\text{Na}_3\text{Li}_3\text{Al}_2\text{F}_{12}(\text{ss})$
38	98	625	Tetragonal phase
39,40	»	630-640	Tetragonal phase + $\delta\text{-Li}_3\text{AlF}_6(\text{ss})$, $a=12.07 \pm 0.01 \text{ \AA}$ (640°C)
41	98	> 650	$\delta\text{-Li}_3\text{AlF}_6(\text{ss})$
42	99	625	$\delta\text{-Li}_3\text{AlF}_6(\text{ss})$, $a=12.04 \pm 0.02 \text{ \AA}$
43	100	625	$\delta\text{-Li}_3\text{AlF}_6$, $a=11.98 \pm 0.01 \text{ \AA}$
44	»	700	$\delta\text{-Li}_3\text{AlF}_6$

Table 2. α - $\text{Na}_2\text{LiAlF}_6$ (20°C). Monoclinic $a=7.538 \pm 0.003$ Å, $b=7.516 \pm 0.003$ Å, $c=7.525 \pm 0.004$ Å, $\beta=90.81 \pm 0.03^\circ$.

<i>hkl</i>	Int.	$\sin^2\theta_{\text{obs.}} \times 10^4$	$\sin^2\theta_{\text{calc.}} \times 10^4$	$d_{\text{calc.}}$
11 $\bar{1}$	vs	311	312	4.366
111	vs	318	318	4.325
200	m	420	418	3.769
00 $\bar{2}$			420	3.762
020			421	3.758
01 $\bar{2}$	w	522	524	3.369
20 $\bar{2}$	m	826	827	2.681
202	s	842	841	2.656
10 $\bar{3}$	m	1042	1041	2.390
103	m	1057	1058	2.370
11 $\bar{2}$	m	1142	1143	2.280
22 $\bar{3}$	vs	1246	1247	2.183
222	vs	1270	1271	2.162
230	m	1363	1365	2.086
12 $\bar{3}$	m	1460 (LiF)	1461	2.017
13 $\bar{2}$	w	1477	1477	2.006
123			1479	2.005
004	vs	1674	1674	1.884
104	w	1773	1772	1.831
23 $\bar{2}$			1773	1.831

vs=very strong, s=strong, m=medium, w=weak.

possible to index all the reflections on a hexagonal basis; and moreover, the agreement between observed and calculated values is far better for the monoclinic cell.

On heating, the monoclinic α - $\text{Na}_2\text{LiAlF}_6$ was transformed to β - $\text{Na}_2\text{LiAlF}_6$, which was found to be cubic *B*-face-centered, with $a=7.639$ Å (445°C). Powder pattern data for β - $\text{Na}_2\text{LiAlF}_6$ are given in Table 3. The transformation from α - $\text{Na}_2\text{LiAlF}_6$ to β - $\text{Na}_2\text{LiAlF}_6$ could not be observed by DTA. By X-ray studies the angle β was found to approach 90° upon heating, and the transformation seemed to be complete at 420°C.

Table 3. β - $\text{Na}_2\text{LiAlF}_6$ (445°C). Cubic, $a=7.639 \pm 0.005$ Å.

<i>hkl</i>	Int.	$\sin^2\theta_{\text{obs.}} \times 10^4$	$\sin^2\theta_{\text{calc.}} \times 10^4$
110	vs	306	306
200	m	406	407
220	m	814	815
310	w	1020	1019
311	m	1122	1120
222	vvs	1222	1222
312	w	1427	1426
400	vs	1629	1630

vvs=very, very strong, vs=very strong, m=medium, w=weak.

The structure of $\beta\text{-Na}_2\text{LiAlF}_6$ is very similar to that of $\beta\text{-Na}_3\text{AlF}_6$, except for some fairly weak additional reflections which are not observed in $\beta\text{-Na}_3\text{AlF}_6$. Because of these reflections, a one-face-centered unit cell must be assigned to $\beta\text{-Na}_2\text{LiAlF}_6$, whereas that of $\beta\text{-Na}_3\text{AlF}_6$ is all-face-centered, space group $Fm\bar{3}m$.²¹

Indexing $\alpha\text{-Na}_2\text{LiAlF}_6$ on the basis of a primitive orthorhombic cell, with $a = 5.290 \text{ \AA}$, $b = 5.363 \text{ \AA}$, $c = 7.520 \text{ \AA}$ also leads to very good agreement between observed and calculated values. This cell is seen to be closely related to that of $\alpha\text{-Na}_3\text{AlF}_6$, which is monoclinic, $a = 5.412 \text{ \AA}$, $b = 5.599 \text{ \AA}$, $c = 7.777 \text{ \AA}$, $\beta = 90.19^\circ$, space group $P2_1/n$.^{10,19,20} This orthorhombic cell for $\alpha\text{-Na}_2\text{LiAlF}_6$ can be seen to be very closely related to the monoclinic cell which we believe to be the correct one. The fact that $\alpha\text{-Na}_2\text{LiAlF}_6$ was found to change gradually to $\beta\text{-Na}_2\text{LiAlF}_6$ upon heating cannot be explained on the basis of an orthorhombic unit cell for $\alpha\text{-Na}_2\text{LiAlF}_6$, and moreover a change from an orthorhombic to a cubic structure should give a heat effect large enough to be observed by DTA. Therefore the monoclinic unit cell is assumed to be the correct one for $\alpha\text{-Na}_2\text{LiAlF}_6$.

d) *The compound $\text{Na}_3\text{Li}_3\text{Al}_2\text{F}_{12}$.* $\text{Na}_3\text{Li}_3\text{Al}_2\text{F}_{12}$ was found to be cubic, $a = 12.127 \text{ \AA}$ (at 20°C), space group $Ia\bar{3}d$. The observed d -values and intensities are in good agreement with those reported by Menzer²² for the mineral cryolithionite. Menzer found the mineral to be cubic, with $a = 12.097 \text{ \AA}$. Cryolithionite has the same structure as grossularite, $\text{Ca}_3\text{Al}_2(\text{SiO}_4)_3$, which belongs to the garnets. From a crystallographic point of view the formula of cryolithionite should therefore be written $\text{Na}_3\text{Al}_2(\text{LiF}_4)_3$.

When Na_3AlF_6 and Li_3AlF_6 in molar proportions 1:1 were fused and cooled off directly (cooling time 4–6 h), reflections from $\alpha\text{-Na}_2\text{LiAlF}_6$ were found in the X-ray diagrams (at room temperature) in addition to the cryolithionite reflections. This has in earlier works^{6,8} been interpreted as an indication that cryolithionite is not stoichiometric $\text{Na}_3\text{Li}_3\text{Al}_2\text{F}_{12}$, but contains an excess of Li_3AlF_6 . However, powder diagrams taken of samples which had been equilibrated at 500°C for 70 h before cooling, showed that pure cryolithionite had been formed.

The lattice of $\text{Na}_3\text{Li}_3\text{Al}_2\text{F}_{12}$ expands fairly rapidly upon heating. At 450°C the lattice constant was 12.27 \AA . At 550°C reflections from $\beta\text{-Na}_2\text{LiAlF}_6$ appeared in addition to those of cryolithionite.

Table 4. Phases present in $\text{Na}_3\text{Li}_3\text{Al}_2\text{F}_{12}$ after equilibration at various temperatures.

Equilibration data		Phases observed at room temperature
Temperature ($^\circ\text{C}$)	Time (hours)	
480–550	69	$\text{Na}_3\text{Li}_3\text{Al}_2\text{F}_{12}$
540–555	75	$\text{Na}_3\text{Li}_3\text{Al}_2\text{F}_{12} + \alpha\text{-Na}_2\text{LiAlF}_6$ (small amounts)
585–600	72	$\text{Na}_3\text{Li}_3\text{Al}_2\text{F}_{12} + \alpha\text{-Na}_2\text{LiAlF}_6$
630–640	36	$\text{Na}_3\text{Li}_3\text{Al}_2\text{F}_{12} + \alpha\text{-Na}_2\text{LiAlF}_6$
680–690	40	$\alpha\text{-Na}_2\text{LiAlF}_6 + \beta\text{-Li}_3\text{AlF}_6$
705–720	33	$\alpha\text{-Na}_2\text{LiAlF}_6 + \beta\text{-Li}_3\text{AlF}_6$

Some samples of the composition $\text{Na}_3\text{Li}_3\text{Al}_2\text{F}_{12}$ were equilibrated at various temperatures, cooled off and then examined by X-ray diffraction. The results of these experiments are given in Table 4. They show that pure $\text{Na}_3\text{Li}_3\text{Al}_2\text{F}_{12}$ is stable up to a little above 500°C . This is in agreement with the results from the high-temperature X-ray studies.

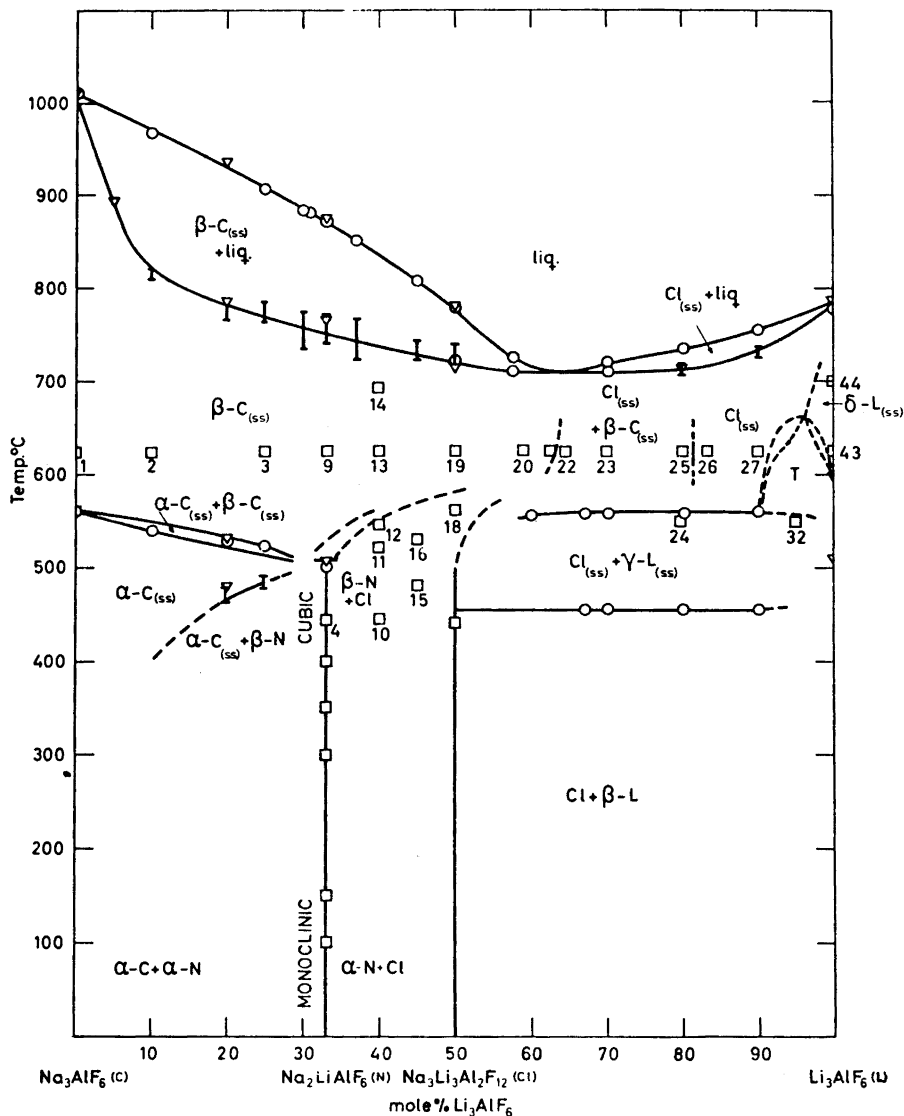


Fig. 3. The phase diagram of the system $\text{Na}_3\text{AlF}_6 - \text{Li}_3\text{AlF}_6$, from this work. O, ∇, Points obtained by DTA. I: Area of phase change, found by DTA. □ Samples studied by X-ray diffraction, (see also Figs. 4 and 5). The numbers refer to Table 1. C denotes sodium cryolite, N $\text{Na}_2\text{LiAlF}_6$, Cl cryolithionite and L lithium cryolite. SS denotes solid solution.

Table 5. Reflections from tetragonal phase in the system Na_3AlF_6 – Li_3AlF_6 at composition 95 mole % Li_3AlF_6 –5 mole % Na_3AlF_6 , temperature 625°C. $a=11.97\pm 0.02$ Å, $c=8.73\pm 0.02$ Å.

hkl	Int.	$\sin^2\theta_{\text{obs.}} \times 10^4$	$\sin^2\theta_{\text{calc.}} \times 10^4$
211	vw	278(LiAl_5O_8)	285
002	m	311	312
	m	321(cubic phase)	
220	vs	327	332
102	vs	343	353
222	s	643(cubic phase)	643
003	s	698	702
330	w	745	747
	vvw	802(cubic phase)	
402	m	979	976
412	w	1024(LiAl_5O_8)	1017
430	w	1041(LiF)	1037
004	vw	1252(cubic phase)	1248
512	w	1389(LiF)	1390
531	w	1489(cubic phase)	1488
611	m	1602(cubic phase)	1612

vs=very strong, s=strong, m=medium, w=weak, vw=very weak, vvw=very, very weak

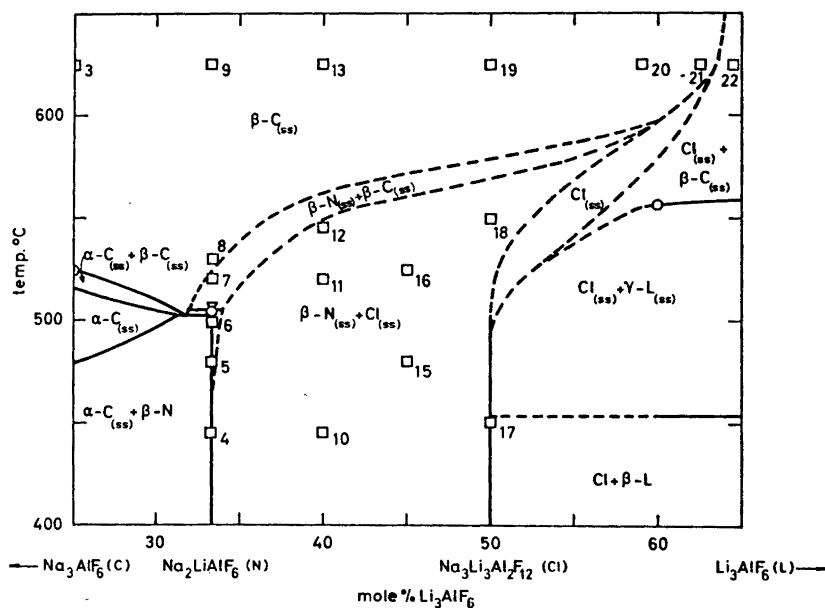


Fig. 4. Section of the phase diagram Na_3AlF_6 – Li_3AlF_6 . For explanation of the symbols, see legend to Fig. 3. Possible situation in areas where not enough data have been obtained has been sketched.

e) *Other phases.* By the high-temperature X-ray examinations, one new phase was found in addition to the various modifications of Na_3AlF_6 , $\text{Na}_2\text{LiAlF}_6$, $\text{Na}_3\text{Li}_3\text{Al}_2\text{F}_{12}$, and Li_3AlF_6 . This phase, which can be indexed on the basis of a tetragonal unit cell, has an area of stability between 560°C and 630°C, from 90 to 99 mole % Li_3AlF_6 . The lattice parameters are $a = 11.97 \text{ \AA}$, $c = 8.73 \text{ \AA}$ (625°C). Powder pattern data for this phase are given in Table 5.

On the basis of our DTA and X-ray examinations we have constructed the phase diagram of the system, as shown in Fig. 3. In Figs. 4 and 5 sections

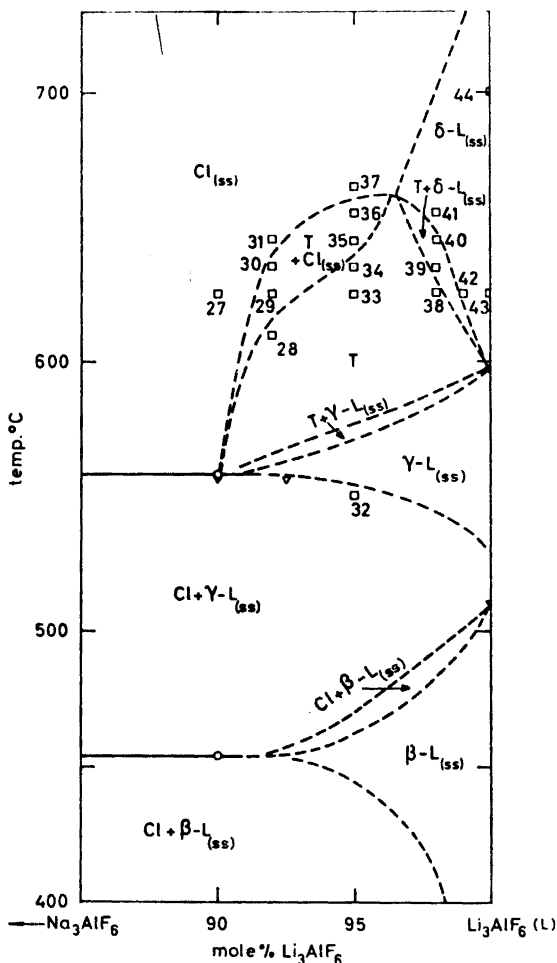


Fig. 5. Section of the phase diagram Na_3AlF_6 - Li_3AlF_6 . For explanation of the symbols, see legend to Fig. 3. Possible situation in areas where not enough data have been obtained has been sketched.

of the phase diagram are given in greater detail. In these figures are also shown suggestions as to the possible situation where this has not been completely clarified by our investigations.

As can be seen there is extensive formation of solid solutions in the system. The solubility of lithium cryolite in solid sodium cryolite is large, and there is little change in the lattice parameter of sodium cryolite with increasing lithium cryolite content. Addition of sodium cryolite to lithium cryolite, however, leads to a marked increase in the lattice constant, and the solubility is restricted to a few per cent. It is clear that whereas a large amount of the small lithium ions can be put into sodium cryolite without changing the structure, only a very limited amount of the larger sodium ions can be accommodated in the lithium cryolite lattice.

Acknowledgements. The authors acknowledge their indebtedness to Professor K. Grjotheim. Thanks are expressed to Professor J. Krogh-Moe, the University of Trondheim, for the use of the high-temperature X-ray camera, and for valuable suggestions. We also wish to thank Professor H. Pauly, the Technical University of Denmark, who initiated these studies. *The Royal Norwegian Council for Scientific and Industrial Research* is thanked for financial support.

REFERENCES

1. Drossbach, P. Z. *Elektrochem.* **42** (1936) 65.
2. Mashovets, V. P. and Petrov, V. I. *Zh. Prikl. Khim.* **30** (1957) 1965; (*J. Appl. Chem. USSR* **30** (1957) 1758).
3. Rolin, M. and Muhlethaler, R. *Bull. Soc. Chim. France* **1964** 2593.
4. Chin, D. A. and Hollingshead, E. A. *J. Electrochem. Soc.* **113** (1966) 736.
5. Babayan, G. G., Edoyan, R. S. and Manvelyan, M. G. *Arm. Khim. Zh.* **20** (1967) 20.
6. Garton, G. and Wanklyn, B. M. *J. Am. Ceram. Soc.* **50** (1967) 395.
7. Malinovský, M., Paučířová, M. and Matiašovský, K. *Chem. Zvesti* **23** (1969) 27.
8. Holm, J. L. *Acta Chem. Scand.* **20** (1966) 1167.
9. Beletskii, M. S. and Saksonov, K. G. *Zh. Neorg. Khim.* **2** (1957) 414; (*Russ. J. Inorg. Chem.* **2** (1957) 284).
10. Holm, J. L. *Undersøkelser av struktur og faseforhold for en del systemer med tilknytning til aluminiumelektrolysen*, Lic. Thesis, Institute of Inorganic Chemistry, NTH, Trondheim 1963.
11. Holm, J. L. and Jenssen, B. *Acta Chem. Scand.* **23** (1969) 1065.
12. Motzfeldt, K. In Bockris, J. O. M., White, J. L. and Mackenzie, J. D. *Physicochemical Measurements at High Temperatures*, Butterworths, London 1960, pp. 47–86.
13. Smith, D. K. *Norelco Repr.* **10** (1963) 19.
14. Jenssen, B. *Fase- og strukturforhold for noen komplekse alkalialuminiumfluorider*, Lic. Thesis, Institute of Inorganic Chemistry, NTH, Trondheim 1969.
15. Kordes, E. Z. *Krist* **91** (1935) 194.
16. Bunk, A. J. H. and Tichelaar, G. W. *Koninkl. Ned. Akad. Wetenschap. Proc. Ser. B* **57** (1954) 73.
17. Barret, W. T. and Wallace, W. E. *J. Am. Chem. Soc.* **76** (1954) 366.
18. Luova, P. and Muurinen, M. *Ann. Univ. Turku. Ser. A I No.* **110** (1967).
19. Náráy-Szabó, St. v. and Sasvári, K. Z. *Krist.* **99** (1938) 27.
20. Ferguson, R. B. *Am. Mineralogist* **34** (1949) 383.
21. Steward, E. G. and Rooksby, H. P. *Acta Cryst.* **6** (1953) 49.
22. Menzer, G. Z. *Krist.* **75** (1930) 265.

Received January 16, 1970.